International Journal of Advances in Engineering and Management (IJAEM)
Volume 5, Issue 12 Dec 2023, pp: 116-130 www.ijaem.net ISSN: 2395-5252

Flow and Heat Transfer of a Fluid-Particle Suspension past a Vertical Exponentially Stretching Surface with Internal Heat Generation/Absorption

Pavithra G.M[1] and Subramanya K[2]

[1]*Department of Mathematics, Sahyadri Science College, Kuvempu University,Shankaraghatta-577 451, Shimoga, Karnataka, INDIA.*

[2]*Department of Physics, Sahyadri Science College, Kuvempu University,Shankaraghatta-577 451, Shimoga, Karnataka, INDIA.*

Date of Submission: 06-12-2023 Date of Acceptance: 16-12-2023

ABSTRACT: This article reports a study on the effect of internal heat generation/absorption and viscous dissipation over an exponentially stretching surface in the presence of a transverse magnetic field on two-dimensional boundary layer steady flow and heat transfer of a viscous incompressible dusty fluid. Choosing the suitable similarity transformations, the governing boundary layer equations are transformed into a set of non-linear ordinary differential equations and solved numerically by Runge-Kutta-Fehlberg 45 scheme with the help of Maple software. Two cases are studied for heat transfer analysis, namely, (i) prescribed exponential order surface temperature (PEST) and (ii) prescribed exponential order heat flux at the sheet (PEHF). The obtained numerical results are compared with the earlier study and are found to be in excellent agreement. The effect of the various parameters entering into the problem on the velocity and temperature profiles are derived, discussed numerically for various values of physical parameters and presented through graphs and tables.

Keywords: Numerical solution; fluid-particle suspension; exponentially stretching sheet; Runge-Kutta-Fehlberg 45 scheme; internal heat generation/absorption.

I. INTRODUCTION

The analysis of boundary layer flow finds applications in different areas such as the aerodynamic extrusion of a plastic sheet, the cooling of a metallic plate in a cooling bath, the boundary layer along material handling conveyers, blood flow problems, textile and paper industries etc. Boundary layer flow driven by a continuously moving solid surface was initiated by Sakiadis [1] and a good amount of literature have been generated on boundary layer flow of Newtonian and non-Newtonian fluids over a linear and nonlinear stretching surface. Crane [2] extended his work by finding the analytical solution for the problem of steady two-dimensional boundary layer flow past a stretching plate.

Later, this problem has been extended to various aspects by considering linear, non-linear, exponential stretching sheets with magneto-hydro dynamic effects, porous sheets, porous media and heat or mass transfer for both steady and unsteady flow cases. Subsequently comprehensive studies have been carried out on exponential stretching sheet by many researchers. Initially, Magyari and Keller [3] considered an exponential stretching model for boundary layer flow with an exponential temperature distribution. The thermal boundary layer flow on an exponentially stretching continuous surface with an exponential temperature distribution in the presence of magnetic field effect was investigated numerically by Al-Odat et al. [4] and they have introduced a local similarity solution of an exponentially stretching surface. Bidin and Nazar [5] numerically solved the boundary layer flow problem over an exponentially stretching sheet by considering thermal radiation effect. Nadeem et al. [6] discussed the boundary layer flow of a Jeffrey fluid over an exponentially stretching surface and they have obtained the analytical solution using homotopy analysis method (HAM). Considering the importance of MHD, thermal radiation and slip effects on permeable boundary layer flow due to an

International Journal of Advances in Engineering and Management (IJAEM)
Volume 5, Issue 12 Dec 2023, pp: 116-130 www.ijaem.net ISSN: 2395-5252

exponentially stretching sheet, Mukhopadhyay [7] and [8] obtain the numerical solution. Recently, the radiation effect on hydromagnetic Newtonian liquid flow due to an exponential stretching sheet was discussed by Kameswaran et al. [9].

The above mentioned investigation deals with the flow and heat transfer only for fluids induced by horizontal stretching sheet. MHD free-convection flows have great significance from the technological point of view for the applications in the fields of stellar and planetary magnetospheres, aeronautics, chemical engineering and electronics. Mixed convection flows are important when the buoyancy forces significantly affect the flow and the thermal fields due to the large temperature difference between the wall and the ambient fluid. One of the early investigations towards a vertical surface was made by Partha et al. [10] and has discussed the viscous dissipation effect for the boundary layer flow over an exponentially stretching sheet and found that the non-dimensional skin friction coefficient increases due to viscous dissipation in the medium. El-Aziz [11] analysed the boundary-layer flow and heat transfer characteristics associated with a heated exponential stretching continuous sheet being cooled by a mixed convection flow. The effect of thermal radiation on hydro-magnetic flow due to an exponentially stretching sheet was carried out by Reddy and Reddy [12]. Dulal Pal [13] studied the mixed convection heat transfer in the boundary layers on an exponentially stretching continuous surface with magnetic field. A study has been carried out to analyze the combined effects of Soret and Dufour on mixed convection flow over an exponentially stretching sheet by Srinivasacharya and Ram Reddy [14]. El-Aziz and Tamer Nabil [15] investigated the analytical solution by Homotopy analysis method for hydromagnetic mixed convection flow past an exponentially stretching sheet with hall current.

The problems of the fluid mechanics involving dust particles arise in many processes of practical importance, such as flow occurs in powder technology, transport of liquid slurries in chemical processing, nuclear processing, in the fields of fluidization, combustion, use of dust in gas cooling systems, centrifugal separation of matter from fluid, petroleum industry, flow in rocket tubes, purification of crude oil, electrostatic precipitation, polymer technology, fluid droplets sprays and in different geophysical situations. The flow concerning the fluid-particle system for the laminar flow of a dusty fluid has been initiated by Saffman [16]. More recently, Gireesha et al. ([17], [18]) have discussed the effect of viscous dissipation and heat source/sink on MHD boundary layer flow and heat transfer of dusty fluid over an unsteady stretching sheet.

Motivated by these investigations, we have concentrated to study the flow and heat transfer characteristics adjacent to a vertical stretching sheet. This problem differs from the above mentioned investigations where the exponential stretching sheet was not taken into the consideration for dusty fluid. The effects over an exponential stretching surface subjected to suction or injection is considered in this article. An ordinary differential equation of order three representing the momentum equation and a second order differential equation corresponding to the energy equation are derived using similarity transformations. Using Runge-Kutta-Fehlberg 45 scheme, the numerical calculations up to the desired level of accuracy were carried out for different values of dimensionless parameters of the problem under consideration for the purpose of illustrating the results graphically.

II. MATHEMATICAL FORMULATION AND SOLUTION OF THE PROBLEM

Consider a steady two-dimensional laminar boundary layer flow and heat transfer of an incompressible viscous dusty fluid near a vertical wall stretching with velocity U_w and temperature distribution T_w. It is assumed that the surface is stretched with exponential velocity $U_w = U_0 e^{(x/L)}$ in quiescent fluid and the surface is maintained at a temperature $T_w = T_1 + T_0 e^{(c_1 x/2L)}$. The x-axis is chosen along the sheet and y-axis normal to it. The flow is generated as a consequence of exponential stretching of the sheet, caused by simultaneous application of equal and opposite forces along the x-axis keeping in which the origin fixed as in the Figure 1. A uniform magnetic field B is assumed to be applied in the y-direction and suction/injection S is applied normal to the sheet.

International Journal of Advances in Engineering and Management (IJAEM)
Volume 5, Issue 12 Dec 2023, pp: 116-130 www.ijaem.net ISSN: 2395-5252

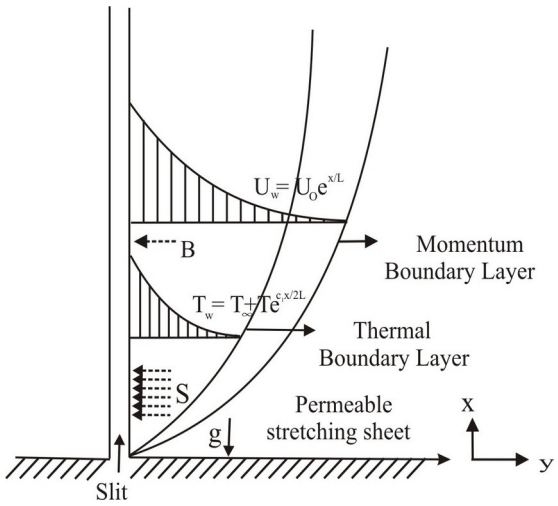

Figure 1: Schematic representation of the boundary layer flow.

Under these assumptions, the two dimensional boundary layer equations can be written as,

$$\frac{\partial u}{\partial x}+\frac{\partial v}{\partial y}=0, \qquad (2.1)$$

$$u\frac{\partial u}{\partial x}+v\frac{\partial u}{\partial y}=\nu\frac{\partial^2 u}{\partial y^2}+\frac{KN}{\rho}(u_p-u), \qquad (2.2)$$

$$\frac{\partial u_p}{\partial x}+\frac{\partial v_p}{\partial y}=0, \qquad (2.3)$$

$$u_p\frac{\partial u_p}{\partial x}+v_p\frac{\partial u_p}{\partial y}=\frac{K}{m}(u-u_p), \qquad (2.4)$$

where and y represents coordinate axes along the continuous surface in the direction of motion and perpendicular to it, respectively. and denotes the velocity components of the fluid and particle phase along the and y directions respectively, T is the temperature of the fluid, T_∞ is the temperature of the fluid far away from the sheet, g is the acceleration due to gravity, β^* is the thermal expansion coefficient, V is the coefficient of viscosity of fluid, is the density of the fluid phase, is the Stoke's resistance, is the number density of dust particles, is the mass concentration of dust particles, is the relaxation time of particle phase and σ is the electrical conductivity.

In order to solve the governing boundary layer equations, consider the following appropriate boundary conditions on velocity,

$$u=U_w(x),\ v=V_w(x) \text{ at } y=0,$$
$$u\to 0,\ u_p\to 0,\ v_p\to 0, \text{as } y\to\infty, \qquad (2.5)$$

where $U_w(x)=U_0e^{(x/L)}$ is the sheet velocity and $V_w(x)=-S\sqrt{U_0\nu/2L}\,e^{(x/2L)}$ is the suction/ injection velocity, U_0 is reference velocity, L is the reference length and S is the suction/injection parameter. It should be noted that $S>0$ corresponds to fluid wall suction while $S<0$ indicates fluid wall injection.

Equations (2.1) to (2.4) are subjected to boundary condition (2.5), admit a self-similar solution in terms of the similarity function f and the similarity variable η as

$$u=U_0e^{\frac{x}{L}}f'(\eta),$$
$$v=-\sqrt{\frac{u_0\nu}{2L}}e^{\frac{x}{2L}}[f(\eta)+\eta f'(\eta)],$$

$$u_p=U_0e^{\frac{x}{L}}F'(\eta),$$
$$v_p=-\sqrt{\frac{u_0\nu}{2L}}e^{\frac{x}{2L}}[F(\eta)+\eta F'(\eta)],$$
$$\eta=\sqrt{\frac{u_0}{2\nu L}}e^{\frac{x}{2L}}y \qquad B=B_0e^{\frac{x}{2L}},$$
$$\theta(\eta)=\frac{T-T_\infty}{T_w-T_\infty}, \qquad (2.6)$$

where B_0 is the magnetic field flux density.

These equations identically satisfy the governing equations (2.1) and (2.2). Substitute equation (2.5) into equations (2.1) and (2.3) and on equating the coefficient of $(x\setminus L)^0$ on both sides one can get

$$f'''(\eta)+f(\eta)f''(\eta)-2f'(\eta)^2+2\beta[F'(\eta)-f'(\eta)]-Mf'(\eta)+2Gr\theta(\eta)=0 \qquad (2.7)$$

$$F(\eta)F''(\eta)-2F'(\eta)^2+2\beta[f'(\eta)-F'(\eta)]=0 \qquad (2.8)$$

where prime denotes the differentiation with respect to and is the mass concentration, is the fluid-particle interaction parameter for velocity,

International Journal of Advances in Engineering and Management (IJAEM)
Volume 5, Issue 12 Dec 2023, pp: 116-130 www.ijaem.net ISSN: 2395-5252

$M = 2\sigma B_0^2 L / \rho U_0$ is the magnetic parameter and $Gr = g\beta(T_w - T_\infty)L/U_0^2$ is the Grashof number.

Using similarity transformations, the boundary conditions (2.4) become

$$f'(\eta)=1,\ f(\eta)=S \text{ at } \eta=0,$$
$$f'(\eta)=0,\ F'(\eta)=0,$$
$$F(\eta)=f(\eta)+\eta f'(\eta)-\eta F'(\eta) \text{ as } \eta\to\infty, \quad (2.9)$$

The important physical parameter for the boundary layer flow is the skin-friction coefficient which is defined as,

$$C_f = \frac{\tau_w}{\rho U_w^2}, \quad (2.10)$$

where the skin friction τ_w is given by,

$$\tau_w = \mu\left(\frac{\partial u}{\partial y}\right)_{y=0}. \quad (2.11)$$

Using the non-dimensional variables, one obtains,

$$\sqrt{2\,\mathrm{Re}\,C_f} = f''(0),$$

where $\mathrm{Re} = \frac{U_0 L}{\nu}$ is the Reynolds number.

III. HEAT TRANSFER ANALYSIS

The governing steady, boundary layer heat transport equations with internal heat generation/absorption and viscous dissipation are given by,

$$\rho c_p\left[u\frac{\partial T}{\partial x}+v\frac{\partial T}{\partial y}\right]=k\frac{\partial^2 T}{\partial y^2}+\frac{Nc_p}{\tau_T}(T_p-T)+\frac{N}{\tau_v}(u_p-u)^2+\mu\left(\frac{\partial u}{\partial y}\right)^2+Q(T-T_\infty), \quad (3.1)$$

$$Nc_m\left[u_p\frac{\partial T_p}{\partial x}+v_p\frac{\partial T_p}{\partial y}\right]=-\frac{Nc_p}{\tau_T}(T_p-T), \quad (3.2)$$

where T and T_p are the temperatures of the fluid and dust particle inside the boundary layer, c_p and are the specific heat of fluid and dust particles, is the thermal equilibrium time i.e., it is time required by a dust cloud to adjust its temperature to the fluid, is the thermal conductivity, τ_v is the relaxation time of the of dust particle i.e., the time required by a dust particle to adjust its velocity relative to the fluid and represents the heat source when $Q>0$ and the sink when .

We have consider the heat transfer phenomenon for two types of heating process, namely

(1) Prescribed exponential order surface temperature (PEST) and

(2) Prescribed exponential order heat flux (PEHF).

Case 1: Prescribed Exponential Order Surface Temperature (PEST):

For this heating process, we employ the following boundary conditions,

$$T = T_w(x) \quad \text{at } y=0,$$
$$T\to T_\infty,\ T_p\to T_\infty \text{ as } y\to\infty, \quad (3.3)$$

where $T_w = T_\infty + T_0 e^{c_1 x/2L}$ is the temperature distribution in the stretching surface, T_0 is a reference temperature and c_1 is a constant.

Introducing the dimensionless variables for the temperatures $\theta(\eta)$ and $\theta_p(\eta)$ as follows:

$$\theta(\eta)=\frac{T-T_\infty}{T_w-T_\infty},\ \theta_p(\eta)=\frac{T_p-T_\infty}{T_w-T_\infty}, \quad (3.4)$$

where $T-T_\infty = T_0 e^{c_1 x/2L}\theta(\eta)$.

Using the similarity variable η and (3.4) into (3.1) and (3.2) and on equating the co-efficient of $(x\setminus L)^0$ on both sides, one can arrive the following system of equations;

$$\theta''(\eta)+\Pr[f(\eta)\theta'(\eta)-c_1 f'(\eta)\theta(\eta)]+\frac{2N}{\rho}\beta_T\Pr[\theta_p(\eta)-\theta(\eta)]$$
$$+\frac{2N}{\rho}\beta\Pr Ec[F'(\eta)-f'(\eta)]^2+\Pr Ec[f''(\eta)]^2+2\Pr\lambda\theta(\eta)=0 \quad (3.5)$$

$$c_1 F'(\eta)\theta_p(\eta)-F(\eta)\theta_p'(\eta)+2\beta_T\gamma[\theta_p(\eta)-\theta(\eta)]=0 \quad (3.6)$$

International Journal of Advances in Engineering and Management (IJAEM)
Volume 5, Issue 12 Dec 2023, pp: 116-130 www.ijaem.net ISSN: 2395-5252

where $\Pr = \mu c_p / k$ is the Prandtl number, $Ec = U_0^2 / c_p T$ is the Eckert number, $\lambda = QL^2 / \mu C_p \,\mathrm{Re}$ is the heat source/sink parameter, $\beta = L / \tau_v U_0$ and $\beta_\tau = L / \tau_T U_0$ are the fluid-particle interaction parameter for velocity and temperature respectively and $\gamma = c_p / c_m$ is the ratio of specific heat.

The corresponding thermal boundary conditions become,

$$\theta(\eta) = 1 \quad \text{at } \eta = 0,$$
$$\theta(\eta) \to 0,\ \theta_p(\eta) \to 0, \text{ as } \eta \to \infty. \quad (3.7)$$

Case 2: Prescribed Exponential Order Heat Flux (PEHF):

For this heating process, the boundary conditions are considered as,

$$\frac{\partial T}{\partial y} = -\frac{q_w(x)}{k} \text{ at } y = 0,$$
$$T \to T_\infty,\ T_p \to T_\infty \text{ as } \eta \to \infty, \quad (3.8)$$

where $q_w(x) = T_1 e^{(\varepsilon_1+1)x/2L}$,

T_1 is reference temperature.

Again using the similarity variable η and equation (3.4) into equations (3.1) and (3.2) and by equating the co-efficient $(x/L)^0$ on both sides, we get the system of equations as in the equations (3.5) and (3.6) with $Ec = kU_0^2 / c_p T_1 \sqrt{U_0 / 2\nu L}$, which is different from the PEST case, and all other parameters are the same as in PEST case.

The corresponding thermal boundary conditions become,

$$\theta'(\eta) = -1 \text{ at } \eta = 0,\ \theta(\eta) \to 0,\ \theta_p(\eta) \to 0, \text{ as } \eta \to \infty \quad (3.9)$$

The important physical parameter for the heat transfer coefficient which is defined as,

$$Nu_x = \frac{x q_w}{k(T_w - T_\infty)}, \quad (3.10)$$

where the heat transfer from the sheet q_w is given by,

$$q_w = -k\left(\frac{\partial T}{\partial y}\right)_{y=0}. \quad (3.11)$$

Using the non-dimensional variables, one obtains,

$$\frac{Nu_x}{\sqrt{2\mathrm{Re}}} = -\frac{x}{2L}\theta'(0) \text{ (PEST case) and}$$
$$\frac{Nu_x}{\sqrt{2\mathrm{Re}}} = -\frac{x}{2L}\frac{1}{\theta(0)} \text{ (PEHF case).}$$

IV. NUMERICAL SOLUTION

The non-linear differential equations (2.6)-(2.7), (3.5)-(3.6) for both PEST and PEHF cases have been solved numerically by applying Runge-Kutta-Fehlberg 45. We have chosen suitable finite value of as

Table 1: Comparison of the results of skin friction coefficient $f''(0)$ for various values of M with $c_1 = 4$ and $\beta = N = S = 0$.

M	Reddy and Reddy [9]	Kameswaran et al. [12]	Present Study
0	-1.28213	-1.28213	-1.28213
1.0	-1.62918	-1.62918	-1.62918
2.0	-	-1.91262	-1.91262
3.0	-	-2.15874	-2.15873
4.0	-	-2.37937	-2.37936

International Journal of Advances in Engineering and Management (IJAEM)
Volume 5, Issue 12 Dec 2023, pp: 116-130 www.ijaem.net ISSN: 2395-5252

Table 2: Comparison of the results of $-\theta'(0)$ for various values of $\Pr$ with $c_1 = 1$ and $\beta = N = S = 0$

$\Pr$	Swati et al. [7]	Mohamed et al. [15]	Present Study
1	0.9547	0.9553	0.9550
2	1.4714	-	1.4714
3	1.8691	1.8693	1.8692
5	2.5001	2.5003	2.5003
10	3.6603	3.6739	3.6603

Tables 1 and 2 provide the values of the skin-friction coefficient and heat transfer coefficient for different values of the magnetic parameter M and Prandtl number $\Pr$. In order to assess the accuracy of the method, the results of $f''(0)$ are compared with those obtained by Reddy and Reddy [9] and Kameswaran et al. [12] in the absence of fluid-particle interaction parameter and Number of dust particles. Also, there is a comparison of our results of $-\theta'(0)$ with Mukhopadhyay et al. [7] and Mohamed et al. [15] as in Table 2 for various values of $\Pr$. From these two tables, one can notice that there is a close agreement with this approach and thus verifies the accuracy of the method used.

Table 3: Values of wall temperature gradient $\theta'(0)$ (for PEST case) and wall temperature $\theta(0)$ (for PEHF case) with $S = 2$.

β	M	Gr	λ	$\Pr$	Ec	N	$-f''(0)$	$\theta'(0)$ (PEST)	$\theta(0)$ (PEHF)
0.2							-1.26625	-0.81099	1.14763
0.6	1.0	1.0	0.5	0.72	0.5	0.5	-1.27862	-0.79106	1.16386
1.0							-1.28809	-0.78371	1.16981
	1.0						-1.27862	-0.79106	1.16386
0.6	2.0	1.0	0.5	0.72	0.5	0.5	-1.61308	-0.67804	1.25833
	3.0						-1.90379	-0.57357	1.35028
		1.0					-1.27862	-0.79106	1.16386
0.6	1.0	2.0	0.5	0.72	0.5	0.5	-0.53159	-0.97643	1.01716
		3.0					0.16055	-1.06425	0.95327
			-0.5				-1.52123	-1.53098	0.71665
0.6	1.0	1.0	0	0.72	0.5	0.5	-1.43730	-1.22788	0.85795
			0.5				-1.27862	-0.79106	1.16386

International Journal of Advances in Engineering and Management (IJAEM)
Volume 5, Issue 12 Dec 2023, pp: 116-130 www.ijaem.net ISSN: 2395-5252

				0.72			-1.27862	-0.79106	1.16386
0.6	1.0	1.0	0.5	1.0	0.5	0.5	-1.38569	-1.01091	0.99324
				1.5			-1.52185	-1.37994	0.82769
					0		-1.32531	-1.00710	0.99394
0.6	1.0	1.0	0.5	0.72	0.5	0.5	-1.27862	-0.79106	1.16386
					1.0		-1.23346	-0.59245	1.30152
						0.5	-1.278623	-0.79106	1.16386
0.6	1.0	1.0	0.5	0.72	0.5	1.0	-1.361391	-0.98772	1.00853
						1.5	-1.420032	-1.14726	0.90725

Further, we have studied the effects of fluid-particle interaction parameter (), magnetic parameter (M), Grashof number (Gr), suction/injection parameter (), heat source/sink parameter (), number density (), Prandtl number () and Eckert number () on velocity and temperature profiles and are depicted graphically. The thermal characteristics at the wall are examined for the values of skin-friction coefficient $f''(0)$, temperature gradient $\theta'(0)$ in PEST case and the temperature $\theta(0)$ in PEHF case are also tabulated in Table 3.

V. RESULTS AND DISCUSSION

For the purpose of discussing the result, the numerical calculations are presented in the form of non-dimensional velocity and temperature profiles. Numerical computations have been carried out for different values of the pertinent parameters. The numerical values are plotted in Figures 2-5 for the velocity profiles and Figures 6-15 for the temperature profiles. We have used the values of $Ec = 0.6$, $M = N = S = 1.0$, $\Pr = 0.72$, $\beta = \beta_T = 0.6$, $c_1 = 1$, $\lambda = 0.5$, $Gr = 2.0$, $\rho = 1$ and $l = 0.1$ throughout our analysis.

Figure 2 reveals the effect of the fluid-particle interaction parameter (β) on the velocity profiles $f'(\eta)$ and $F'(\eta)$. It is noticed from this figure that the velocity profiles decrease with increasing values of β for the fluid phase and increase for the dust phase in the boundary layer. The effect of increasing the values of β is to reduce the velocity $f'(\eta)$ and thereby increase the boundary layer thickness as in Figure 2. In Figure 3, the velocity profiles are drawn for different values of the suction/injection parameter (S). It is observed that the velocity decreases significantly with increasing values of the suction parameter whereas it increases with the injection for both the fluid and dust phases so that the momentum boundary layers become thinner.

International Journal of Advances in Engineering and Management (IJAEM)
Volume 5, Issue 12 Dec 2023, pp: 116-130 www.ijaem.net ISSN: 2395-5252

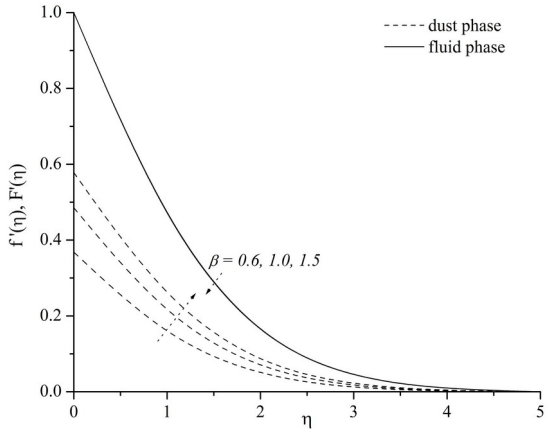

Figure 2: Effect of β on velocity profiles

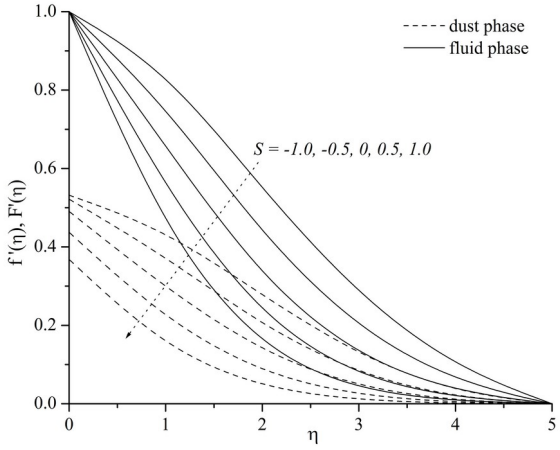

Figure 3: Effect of S on velocity profiles.

The effect of the magnetic parameter (M) on the velocity profiles for the fluid and dust phases are plotted in Figure 4. It explains that as the magnetic field parameter (M) increases, the velocity profile decreases. This is due to the fact that, the introduction of a transverse magnetic field (normal to the flow direction) has a tendency to create a drag, known as the Lorentz force which results in resisting the flow. Figure 5 exhibits the velocity profiles for various values of the Grashof number (Gr). From this figure, we see that the momentum boundary layer thickness reduces due to the increase of the velocity profile for an increase in the Grashof number (Gr).

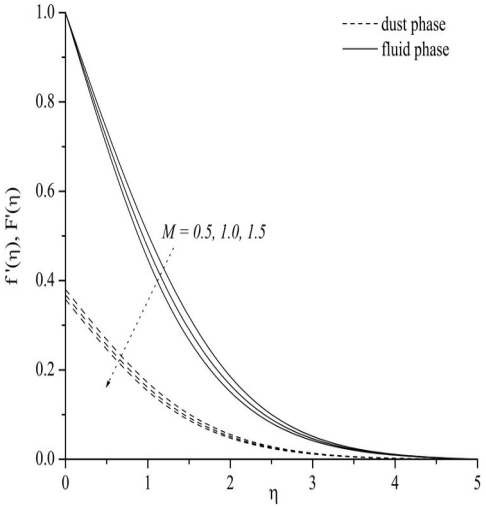

Figure 4: Effect of M on velocity profiles.

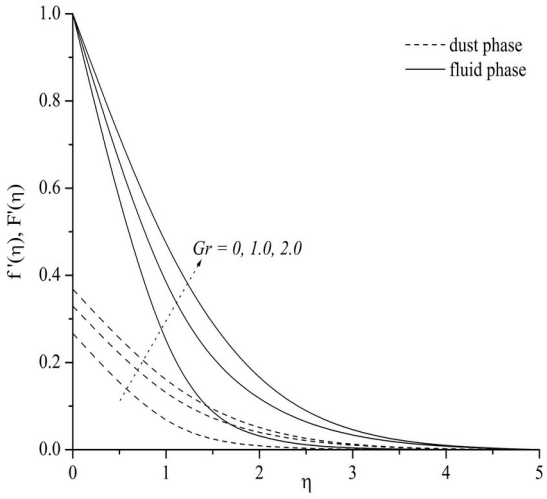

Figure 5: Effect of Gr on velocity profiles.

International Journal of Advances in Engineering and Management (IJAEM)
Volume 5, Issue 12 Dec 2023, pp: 116-130 www.ijaem.net ISSN: 2395-5252

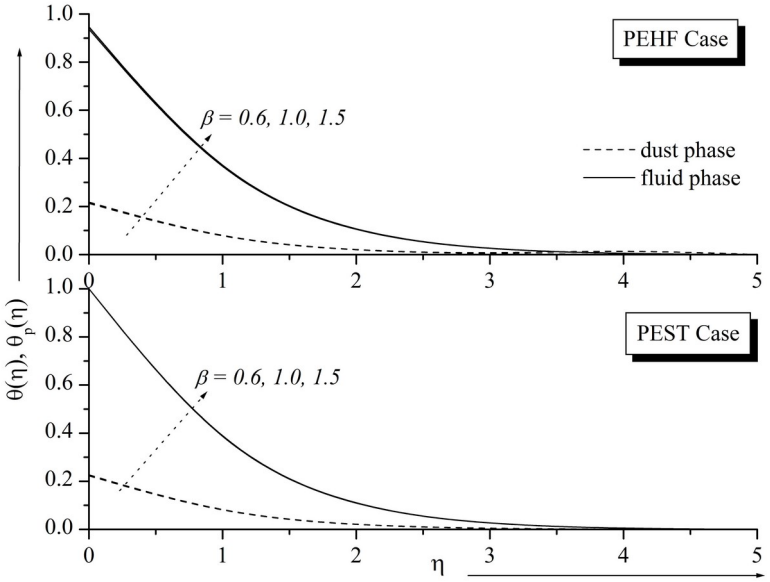

Figure 6: Effect of β on temperature profiles for PEST & PEHF cases.

The temperature profiles for different values of the fluid-particle interaction parameter (β) for both PEST and PEHF cases are presented in Figure 6. This figure shows that there is an increase in the temperature as the fluid-particle interaction parameter (β) increases. The effect of the magnetic field parameter (M) on the temperature profiles $\theta(\eta)$ and $\theta_p(\eta)$ for both PEST and PEHF cases are depicted as in Figure 7. From this figure, we observe that the temperature profiles increase with increases in the magnetic field parameter and also it indicates that both the fluid and the dust phase temperatures are parallel to each other. This is true for both PEST and PEHF cases.

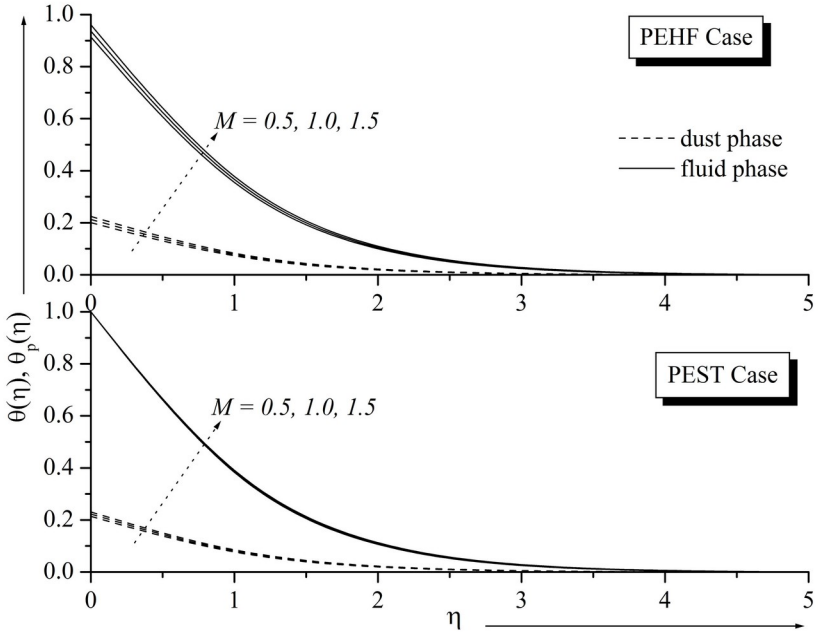

Figure 7: Effect of M on temperature profiles for PEST & PEHF cases.

The variation in the temperature for different values of the Grashof number (Gr) for PEST and PEHF cases are plotted in Figure 8. It is noted that when the Grashof number Gr = 0, the

International Journal of Advances in Engineering and Management (IJAEM)
Volume 5, Issue 12 Dec 2023, pp: 116-130 www.ijaem.net ISSN: 2395-5252

flow becomes a forced convection flow and when the value of Gr increases, the temperature profiles decrease in both cases, and this results in decreasing the thermal boundary layer thickness and the flow becomes a free convection flow.

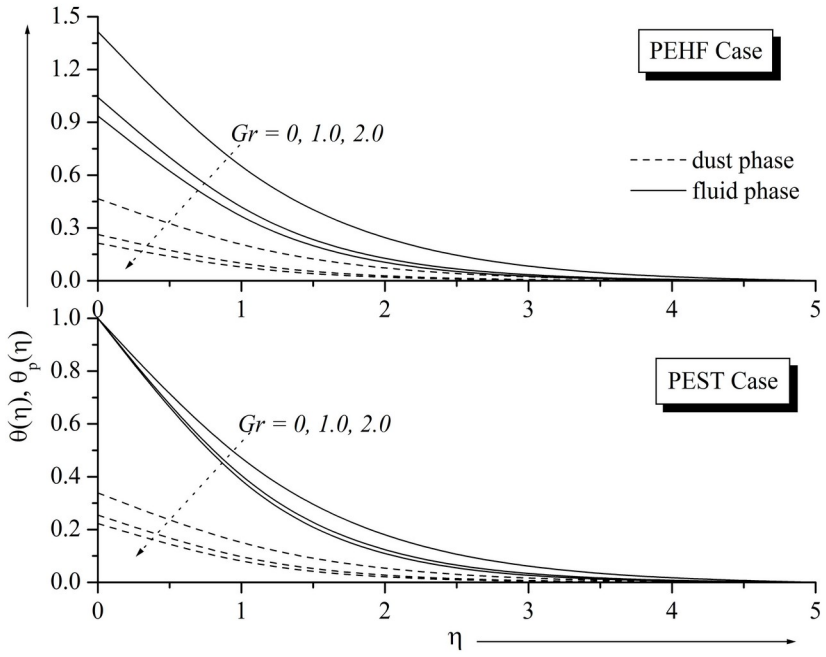

Figure 8: Effect of Gr on temperature profiles for PEST & PEHF cases.

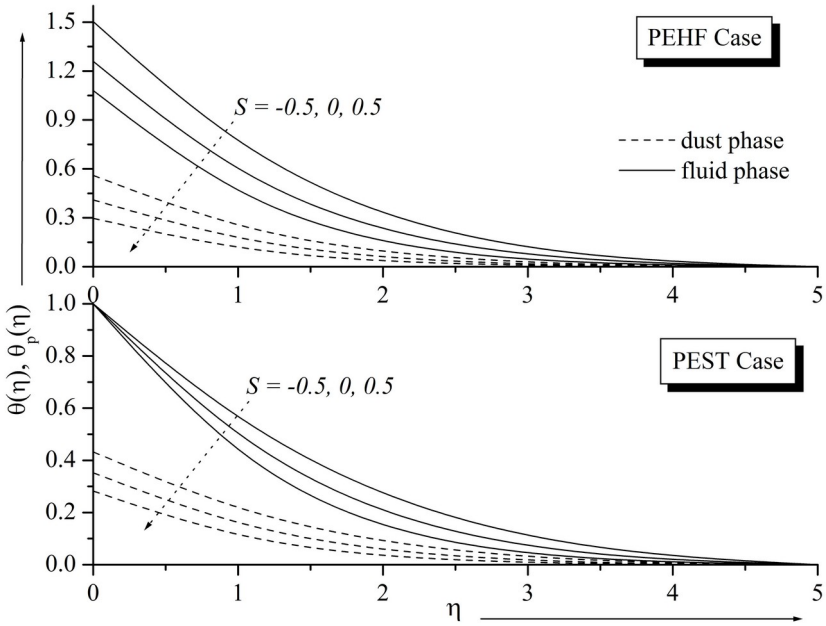

Figure 9: Effect of S on temperature profiles for PEST & PEHF cases.

Figure 9 presents the effect of the suction/injection parameter (S) on the temperature profiles for both PEST and PEHF cases. It reveals that the temperature decreases as the suction parameter increases which results in thinning of the thermal boundary layer thickness. However, by increasing the values of the injection parameter, the temperature increases with an increase in the thermal boundary layer thickness. Hence, suction can be used as a means for cooling the surface as it enhances the heat transfer coefficient much better

International Journal of Advances in Engineering and Management (IJAEM)
Volume 5, Issue 12 Dec 2023, pp: 116-130 www.ijaem.net ISSN: 2395-5252

than injection and thereby the thickness of the thermal boundary layer is reduced.

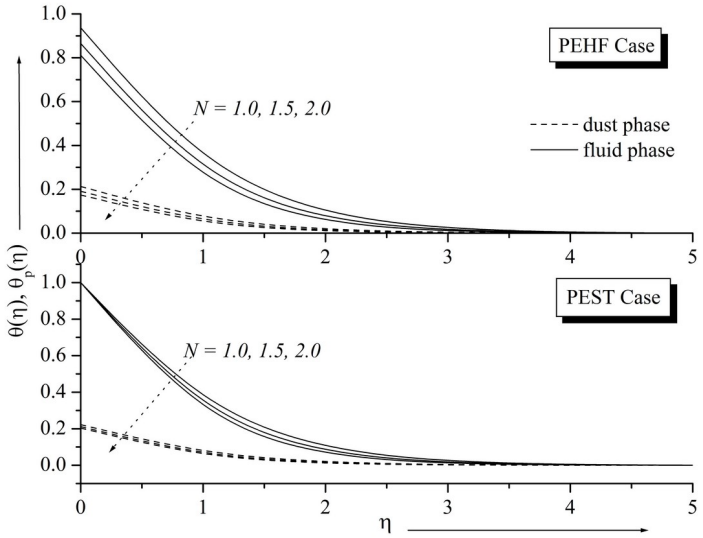

Figure 10: Effect of N on temperature profiles for PEST & PEHF cases.

Figure 10 shows the temperature distributions $\theta(\eta)$ and $\theta_p(\eta)$ for different values of the number density (N). We infer from this figure that the temperature decreases with increases in N for both cases. The effects of the heat source/sink parameter λ on the temperature profiles are observed in Figure 11. It shows that as λ increases, the temperature profiles for both the fluid and the dust phases increase for both PEST and PEHF cases.

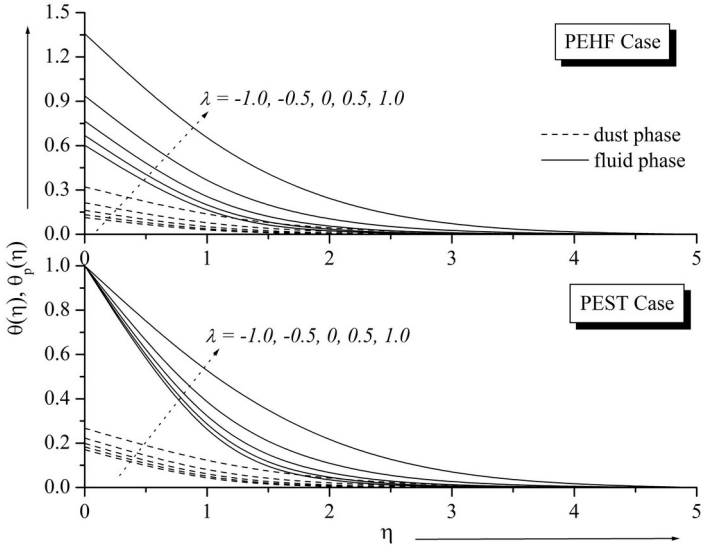

Figure 11: Effect of λ on temperature profiles for PEST & PEHF cases.

Figure 12 exhibits the role of the Prandtl number ($\Pr$) on the temperature profiles for both PEST and PEHF cases. In heat transfer problems, the Prandtl number controls the relative thickness of the momentum and thermal boundary layers. When $\Pr$ is small, it means that the heat diffuses very quickly when compared to the velocity (momentum). This means that for liquid metals the thickness of the thermal boundary layer is much bigger than the velocity boundary layer. Therefore, increasing the value of $\Pr$ results in a decrease in the temperature distribution and hence, the thermal

International Journal of Advances in Engineering and Management (IJAEM)
Volume 5, Issue 12 Dec 2023, pp: 116-130 www.ijaem.net ISSN: 2395-5252

boundary layer thickness decreases as $\Pr$ increases.

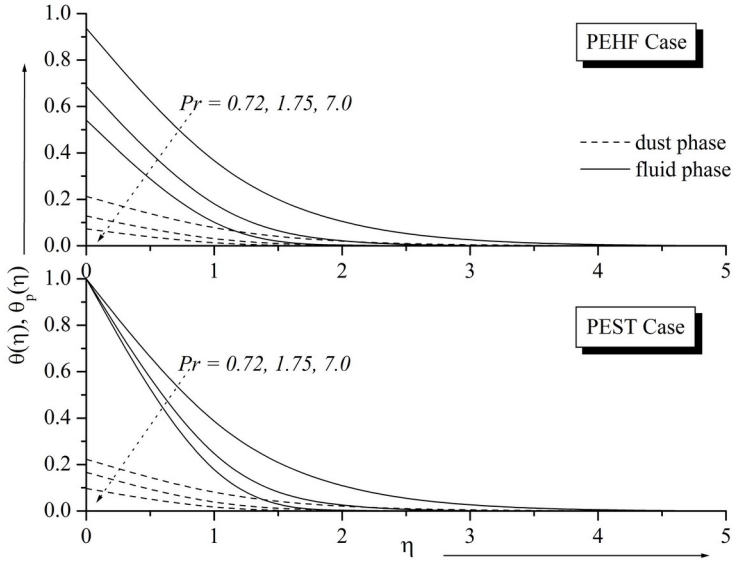

Figure 12: Effect of $\Pr$ on temperature profiles for PEST & PEHF cases.

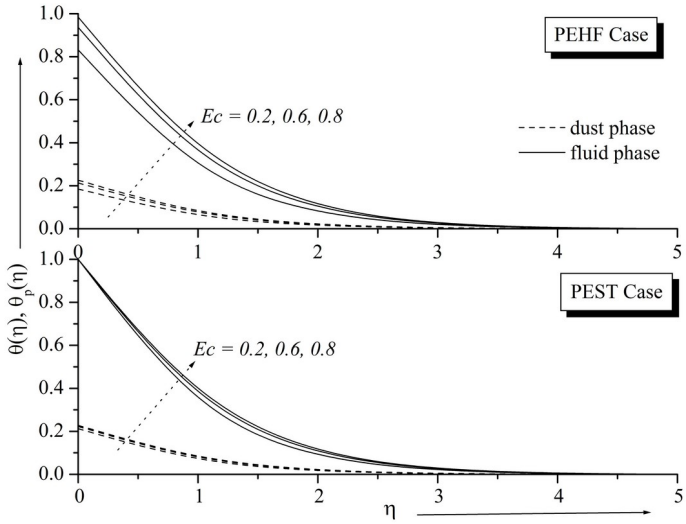

Figure 13: Effect of Ec on temperature profiles for PEST & PEHF cases.

Figure 13 depicts the effect of the Eckert number (Ec) on the temperature profiles with η. It can be seen from this figure that the temperature increases with increasing values of Ec because it plays a role like an energy source, which leads to affect the heat transfer rate. This is due to the heat energy stored in the liquid due to the frictional heating.

Figure 14 shows the variation of the skin friction $f''(0)$ verses the suction/injection parameter S for different values of the magnetic parameter (M) and the Grashof number (Gr), respectively. It can be noticed that the skin friction decreases with an increase in the magnetic parameter (M) and vice versa for the Grashof number (Gr).

International Journal of Advances in Engineering and Management (IJAEM)
Volume 5, Issue 12 Dec 2023, pp: 116-130 www.ijaem.net ISSN: 2395-5252

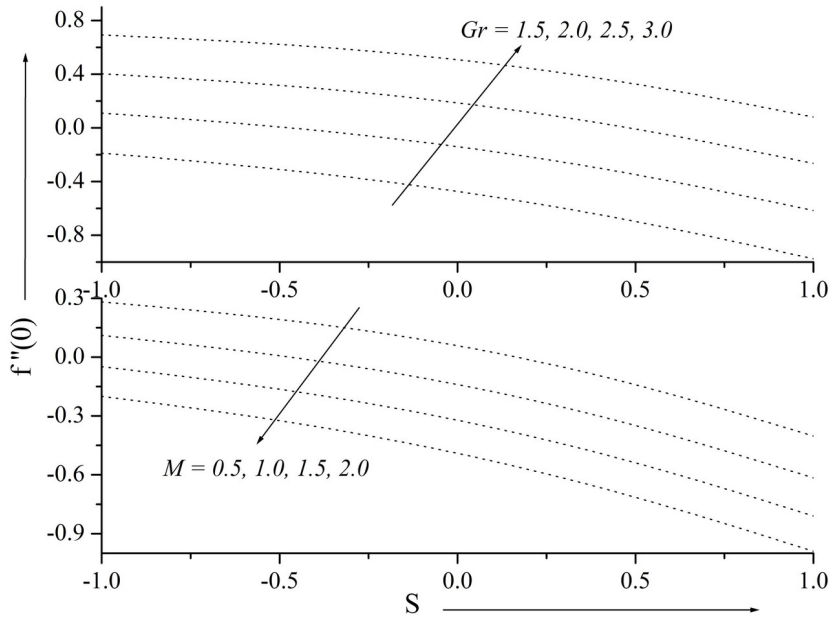

Figure 14: Effect of skin friction coefficient for different values of M and Gr vs S.

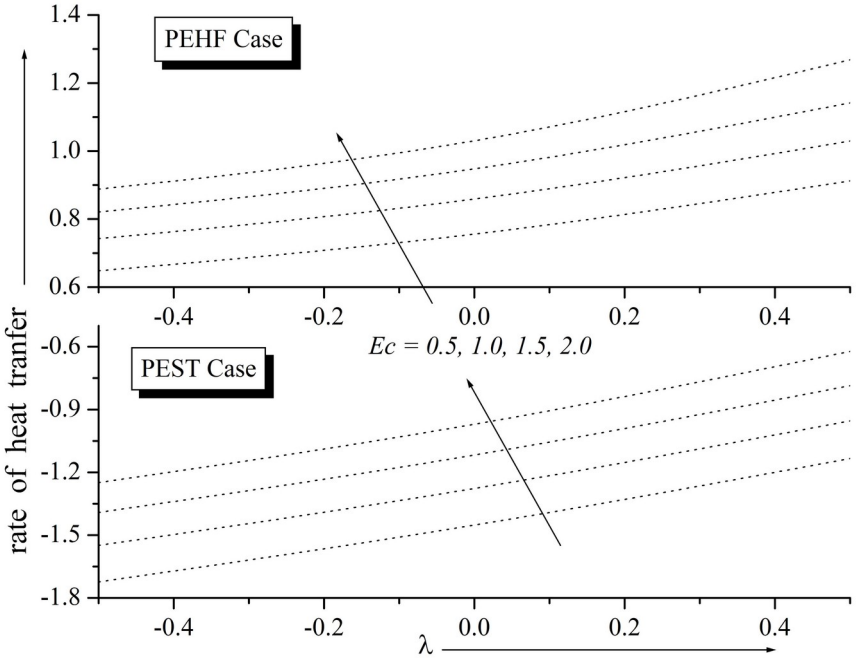

Figure 15: Effect of heat transfer on λ for PEST & PEHF cases.

The rate of heat transfer from the sheet is evaluated by the variation of temperature gradient function $\theta'(0)$ in PEST case and the temperature function $\theta(0)$ in PEHF case and is presented in Figure 15 for various values of Ec. It is observed from this figure that the rate of heat transfer increases with increases in Ec. It is also evident that $\theta'(0)$ is negative which means heat transfer and $\theta(0)$ is positive means heat absorption. Hence, a PEHF case is better suited for cooling process and this is also clear from Table 3.

VI. CONCLUSIONS

A numerical study is performed to study the problem of hydromagnetic flow of an incompressible viscous dusty fluid over an exponentially stretching sheet in the presence of internal heat generation/absorption. The boundary layer equations governing the flow are reduced to

ordinary differential equations using similarity transformations. Using a numerical technique, these equations are then solved to obtain the velocity and temperature distributions as well as the skin-friction coefficient and the Nusselt number for various flow parameters. The results obtained are compared with previously existing results and found to be in good agreement. The major findings from the present study can be summarized as follows:

- The fluid-phase temperature is higher than the dust-phase temperature both in PEST and PEHF cases.
- The velocity profile decreases for increasing values of the suction parameter and the magnetic parameter, but this trend is reversed for increasing values of the Grashof number.
- The effect of the fluid-particle interaction parameter is favourable for the dust-phase velocity and unfavourable for fluid-phase velocity.
- The combined and individual effects of the magnetic parameter, fluid-particle interaction parameter, heat source/sink parameter and the viscous dissipation parameter increase the heat transfer rates.
- The effect of the Grashof number on the temperature field is quite opposite to that of the velocity field.
- Fluid wall suction can be used for cooling the surface.
- The rate of heat transfer decreases due to the effects of N and $\Pr$.
- The skin friction decreases with an increase in M and vice versa for Gr.
- It is observed that $\theta'(0)$ is negative which means heat transfer and $\theta(0)$ is positive means heat absorption. Hence the PEHF case is better for cooling purpose.

REFERENCES:

[1] Sakiadis.B.C, Boundary layer behaviour on continuous solid surface ii, boundary layer behaviuor on continuous flat surface, AIChE J., 7(2) (1961) 221-235.

[2] Crane.L.J, Flow past a stretching plate, Z. Angew. Math. Phy., 21(4) (1970) 645-647.

[3] Magyari.E and Keller.B, Heat and mass transfer in the boundary layers on an exponentially stretching continuous surface, J. Phys. D: Appl. Phys., 32 (1999) 577-585.

[4] Al-Odat.M.Q, Damseh.R.A and Al-Azab.T.A, Thermal boundary layer on an exponentially stretching continuous surface in the presence of magnetic field effect, Int. J. of Appl. Mech. Eng., 11(2) (2006) 289-299.

[5] Biliana Bidin and Roslinda Nazar, Numerical solution of the boundary layer flow over an exponentially stretching sheet with thermal radiation, Eur. J. Sci. Res., 33 (4) (2009) 710-717.

[6] Sohail Nadeem, Shehla Zaheer and Tiegang Fangand, Effects of thermal radiation on the boundary layer flow of a Jeffrey fluid over an exponentially stretching surface, Numer. Algor., 57 (2011) 187-205.

[7] Swati Mukhopadhyay and Rama Subba Reddy Gorla, Effects of partial slip on boundary layer flow past a permeable exponential stretching sheet in presence of thermal radiation, Heat Mass Transfer, 48 (2012) 1773-1781.

[8] Swati Mukhopadhyay, Slip effects on MHD boundary layer flow over an exponentially stretching sheet with suction/blowing and thermal radiation, Ain Shams Engineering Journal (Article in press), (2012).

[9] Kameswaran.P.K, Narayana.M, Sibanda.P and Makanda.G, On radiation effects on hydromagnetic Newtonian liquid flow due to an exponential stretching sheet, Boundary Value Problems, 1(105) (2012) 1-16.

[10] Partha.M.K, Murthy.P.V.S.N and Rajasekhar.G.P, Effect of viscous dissipation on the mixed convection heat transfer from an exponentially stretching surface, Heat and Mass Transfer, 41 (2005) 360-366.

[11] El-Aziz.M.A, Viscous dissipation effect on mixed convection flow of a micropolar fluid over an exponentially stretching sheet, Can. J. Phys., 87 (2009) 359-368.

[12] Bala Anki Reddy.P and Bhaskar Reddy.N, Thermal radiation effects on hydro-magnetic flow due to an exponentially stretching sheet, Int. J. of Appl. Math. Comput., 3(4) (2011) 300-306.

[13] Dulal Pal, Mixed convection heat transfer in the boundary layers on an exponentially stretching surface with magnetic field, Appl. Math. Comput., 217 (2010) 2356-2369.

[14] Srinivasacharya.D and Ch.RamReddy, Soret and dufour effects on mixed convection from an exponentially stretching surface, Int. J. of Nonlinear Science, 12(1) (2011) 60-68.

[15] Mohamed Abd El-Aziz and Tamer Nabil, Homotopy analysis solution of hydromagnetic mixed convection flow past an exponentially stretching sheet with hall current, Math. Probl. Eng., 2012 (2012) 26 pages.

[16] Saffman.P.G, On the stability of laminar flow of a dusty gas, J. Fluid Mechanics, 13 (1962) 120-128.

[17] Gireesha B.J, Chamkha A.J, Manjunatha.S and Bagewadi C.S, Mixed convective flow of a dusty fluid over a vertical stretching sheet with non-uniform heat source/sink and radiation, Int. J. Numer. Meth. Heat Fluid Flow, 23(4) (2013) 598-612.

[18] Gireesha.B.J, Roopa.G.S and Bagewadi.C.S, Effect of viscous dissipation and heat source on flow and heat transfer of dusty fluid over unsteady stretching sheet, Appl. Math. Mech. -Engl. Ed., 33(8) (2012) 1001-1014.